Received: 15 January 2019 | Revised: 17 April 2019 | Accepted: 17 April 2019

DOI: 10.1111/cas.14030

ORIGINAL ARTICLE

WILEY Cancer Science

Structural and functional characterization of β_2-glycoprotein I domain 1 in anti-melanoma cell migration

Shr-Jeng Jim Leu[1,2] | Tzong-Yi Lee[3] | Shu-Wei Cheng[4] | Meng-Ying Tsai[4] | Yu-Shan Lin[4] | Tzeon-Jye Chiou[5] | Kai-Yao Huang[3] | An-Na Chiang[4]

[1]Department of Biotechnology and Laboratory Science in Medicine, National Yang-Ming University, Taipei, Taiwan

[2]Department of Education and Research, Taipei City Hospital, Taipei, Taiwan

[3]Warshel Institute for Computational Biology, Chinese University of Hong Kong, Shenzhen, China

[4]Institute of Biochemistry and Molecular Biology, National Yang-Ming University, Taipei, Taiwan

[5]Division of Transfusion Medicine, Taipei Veterans General Hospital, and School of Medicine, National Yang-Ming University, Taipei, Taiwan

Correspondence
An-Na Chiang, Institute of Biochemistry and Molecular Biology, National Yang-Ming University, Taipei, Taiwan.
Email: anchia@ym.edu.tw

Funding information
Ministry of Science and Technology, Taiwan, Grant/Award Number: MOST103-2320-B-010-024-MY3, MOST106-2320-B-010-028 and MOST107-2320-B-010-035

Abstract

We previously found that circulating β_2-glycoprotein I inhibits human endothelial cell migration, proliferation, and angiogenesis by diverse mechanisms. In the present study, we investigated the antitumor activities of β_2-glycoprotein I using structure-function analysis and mapped the critical region within the β_2-glycoprotein I peptide sequence that mediates anticancer effects. We constructed recombinant cDNA and purified different β_2-glycoprotein I polypeptide domains using a baculovirus expression system. We found that purified β_2-glycoprotein I, as well as recombinant β_2-glycoprotein I full-length (D12345), polypeptide domains I-IV (D1234), and polypeptide domain I (D1) significantly inhibited melanoma cell migration, proliferation and invasion. Western blot analyses were used to determine the dysregulated expression of proteins essential for intracellular signaling pathways in B16-F10 treated with β_2-glycoprotein I and variant recombinant polypeptides. Using a melanoma mouse model, we found that D1 polypeptide showed stronger potency in suppressing tumor growth. Structural analysis showed that fragments A and B within domain I would be the critical regions responsible for antitumor activity. Annexin A2 was identified as the counterpart molecule for β_2-glycoprotein I by immunofluorescence and coimmunoprecipitation assays. Interaction between specific amino acids of β_2-glycoprotein I D1 and annexin A2 was later evaluated by the molecular docking approach. Moreover, five amino acid residues were selected from fragments A and B for functional evaluation using site-directed mutagenesis, and P11A, M42A, and I55P mutations were shown to disrupt the anti-melanoma cell migration ability of β_2-glycoprotein I. This is the first study to show the therapeutic potential of β_2-glycoprotein I D1 in the treatment of melanoma progression.

KEYWORDS

anti-melanoma cell migration, melanoma growth, protein structure analysis, recombinant β_2-glycoprotein I polypeptide domain, site-directed mutagenesis

1 | INTRODUCTION

β_2-Glycoprotein I (β_2-GPI) is a plasma glycoprotein comprising 326 amino acids arranged in five consensus repeat domains.[1] The first four domains of β_2-GPI each contain 60 amino acids, whereas the fifth domain contains an extra 22 amino acids with a lysine-rich positively charged region at the C-terminal extension.[2] β_2-GPI displays multiple effects in antiphospholipid syndrome, autoimmune disorders, vascular thrombosis, coagulation cascade, and oxidative stress.[3-8] Nevertheless, the exact role of each β_2-GPI domain and its structure-function relationships remains unclear.

We previously showed that β_2-GPI plays an essential role in the suppression of vascular endothelial cell growth, cell migration, and angiogenesis under the regulation of nuclear factor-kappa B (NF-κB) signaling and vascular endothelial growth factor (VEGF)-mediated phosphorylation of VEGFR2, ERK1/2 and Akt pathways.[9-11] It is well established that abnormal cell migration and proliferation are closely related to carcinogenesis.[12-15] Furthermore, many studies have reported that inhibition of cell migration decreases tumor growth in multiple cancers.[16-18] Therefore, it is important to elucidate the cellular basis and molecular mechanisms of β_2-GPI function in antitumorigenesis. The present study aims to explore the specific regulatory domain and intracellular signaling of β_2-GPI with a potential for anti-melanoma progression.

Melanoma is one of the most prevalent cancers and the incidence rate of melanoma skin cancer is increasing worldwide.[19-21] Therefore, development of new strategies to prevent and treat melanoma is crucial. The present study investigated the function and structural characteristics of purified β_2-GPI and its recombinant polypeptides in melanoma cell migration, proliferation and invasion, as well as the effects on melanoma growth in vivo. We also identified the specific amino acid residues of β_2-GPI involved in the inhibition of melanoma cell malignancy. This is the first study to show that purified β_2-GPI and its D1 domain inhibit melanoma cell migration, proliferation, and invasion in vitro and reduce melanoma growth in vivo. Moreover, the amino acid residues within the D1 domain for the function of anti-melanoma cell migration was also determined. This study has advanced our knowledge of the structure-function relationship of β_2-GPI D1 in control of melanoma development.

2 | MATERIALS AND METHODS

2.1 | Cell culture

B16-F10 murine melanoma cells were purchased from the Bioresource Collection and Research Center, Taiwan and cultured in DMEM supplemented with 10% heat-inactivated FBS and 1% penicillin/streptomycin/amphotericin B. Cells were seeded in 6-well plates at a density of 1.8×10^5 cells/well and treated with the indicated concentrations of purified β_2-GPI, recombinant D1, D4, D5, D1234, and D12345 polypeptides, Fc vector, and BSA (control). All B16-F10 cells were maintained at 37°C in a humidified atmosphere of 5% CO_2.

2.2 | Purification of β_2-GPI and recombinant β_2-GPI polypeptides

β_2- Glycoprotein I was purified from human plasma using an established protocol.[9] Briefly, plasma β_2-GPI was isolated by 3% perchloric acid precipitation followed by heparin-sepharose affinity chromatography (HiTrap Heparin; GE Healthcare Bio-Sciences, Marlborough, MA, USA). Purity of β_2-GPI was confirmed by SDS-PAGE and western blot analysis.

A Bac-to-Bac Baculovirus Expression System (Thermo Fisher Scientific, Waltham, MA, USA) was used to obtain baculovirus expressing recombinant β_2-GPI polypeptides. Human β_2-GPI cDNAs were cloned into a modified pFastBac1 vector using sense primers with an *Spe*I restriction site and antisense primers with a *Kpn*I restriction site (primer sequences are shown in Table S1). Figure S1A provides details of the β_2-GPI-expressing constructs. The N-terminal dual tag was removed by TEV protease cleavage. Baculovirus stocks expressing β_2-GPI were used to infect SF9 insect cells according to the manufacturer's procedures (Life Technologies, Thermo Fisher Scientific). Expressed polypeptides were purified by affinity purification using a Protein A column (Agarose bead technologies, Doral, FL, USA). The purity of recombinant polypeptides was verified by Coomassie Brilliant blue staining as well as by western blot analysis (Figure S1B).

2.3 | Wound-healing assay

Wound-healing assays were carried out using the tip of a 1-mL micropipette to make a straight scratch on a confluent monolayer of B16-F10 cells in a 6-well plate. Then, the cells were rinsed twice using PBS before adding the indicated concentrations of purified β_2-GPI, recombinant D1, D4, D5, D1234, and D12345 polypeptides at 0 and 24 hours. Representative images of melanoma cell migration were photographed using an inverted phase microscope (Model IX70; Olympus, Tokyo, Japan). For all treatments, the wound at 0 hour was assigned as 100% and was compared with the percentage of wound healing at 24 hours. Photographs were taken using more than three fields per well and ImageJ software was used to calculate wound areas.

2.4 | Transwell migration assay

A 24-well culture plate with a Millicell insert (Millipore, Burlington, MA, USA) was used to carry out transwell migration. A total of 5×10^4 B16-F10 cells were plated into inserts in 0.5 mL medium containing 2% FBS and incubated for 24 hours at 37°C. The lower chamber was filled with complete DMEM medium supplemented with 10% FBS to induce cell migration. Cells that had traversed the membrane were fixed with 4% paraformaldehyde for 15 minutes, washed once using PBS, and stained using 0.5% crystal violet for 45 minutes. To assess cell migration, photographs were taken in more than five fields per membrane. The cells were counted under a microscope and were analyzed using ImageJ software. Changes in cell migration were expressed as a percentage of the control group by at least three independent experiments.

2.5 | Cell proliferation assay

B16-F10 cells were seeded at a density of 1.5×10^5 cells per well in 6-well plates and incubated overnight. Then, the cells were cultured for another 24, 36, or 48 hours in the presence or absence of purified β_2-GPI, various recombinant β_2-GPI polypeptides, Fc, or BSA. Number of viable cells was evaluated by staining with 0.4% Trypan blue (Invitrogen, Carlsbad, CA, USA), and directly counting the number of cells under a microscope.

Cell proliferation was also assessed by BrdU proliferation assay. A total of 2×10^4 cells were seeded on 96-well plates and incubated with purified β_2-GPI, various recombinant β_2-GPI polypeptides, Fc, or BSA for 24 hours. After labeling with 10 μmol/L BrdU for 2 hours, cells were fixed using FixDenat for 30 minutes, blocked with 5% BSA for 30 minutes, and incubated with anti-BrdUPOD monoclonal antibody at room temperature for 90 minutes. Incorporation of BrdU was measured using an ELISA colorimetric kit (Roche Applied Science, Penzberg, Germany) according to the manufacturer's instructions. All assays were done in triplicate.

2.6 | Cell invasion assay

Cell invasion assays were carried out using a 24-well culture plate with a millicell insert (Millipore) coated with 7% Matrigel matrix GFR (Corning, New York, NY, USA). A total of 5×10^4 transfected melanoma cells were seeded in DMEM supplemented with 2% FBS in the upper chamber, and DMEM supplemented with 10% FBS in the lower chamber. The cells were cultured for 24 hours at 37°C; then, the cells in the lower chamber were fixed with 4% paraformaldehyde and stained with 0.5% crystal violet. Excess dye was rinsed with water until the background was clear. The cells were then counted under an inverted microscope in five randomly selected fields.

2.7 | Western blot analysis

Western blot analysis was carried out as previously described.[11] In brief, cells were lysed in RIPA buffer and cell extracts were separated by centrifugation at 12 000 *g* for 20 minutes at 4°C. Nuclear extracts were prepared for analysis of nuclear p50 and p65 levels. The proteins were separated on a 10% SDS polyacrylamide gel and transferred to a PVDF membrane (Millipore). Immunoblots were blocked with 5% non-fat milk and then probed with primary antibodies against p-AKT, AKT p-ERK, ERK, p-p38, p38, p-JNK, JNK, β-actin, p-IKKα, IKKα, p-IκBα, IκBα, p50, p65, lamin A/C, and α-tubulin overnight at 4°C. After washing, transferred blots were incubated with HRP-conjugated secondary antibodies at room temperature for 2 hours. Bound IgG protein bands were visualized using an ECL detection system (BioRad Laboratories, Hercules, CA, USA) and quantified by densitometry using Image Quant software (Molecular Dynamics). Expression of each protein was normalized to the expression level of β-actin (for cytosolic proteins) or lamin A/C (for nuclear proteins).

2.8 | In vivo antitumor study

C57B/6 mice were obtained from the National Laboratory Animal Center, Taiwan, and maintained in the animal center at National Yang-Ming University. The Animal Care and Use Committee of National Yang-Ming University approved all the procedures. Mice were randomly assigned to five different groups. B16-F10 cells were grown in DMEM supplemented with 10% FBS until they reached 80% confluence. The cells were harvested using trypsin-EDTA and resuspended in FBS-free medium. A total of 5×10^6 cells (in 250 μL medium) were injected s.c. into the dorsal surface of four 8-week-old male C57B/6 mice for each group. Tumor development was measured using a Vernier caliber. Tumor volume was measured using the formula: volume (mm^3) = $a \times (b)^2 \times 0.5$, where *a* (mm) and *b* (mm) represent the longest and shortest dimensions of the tumor, respectively. Once the tumor volumes reached approximately 100 mm^3, 250 μL purified β_2-GPI or recombinant β_2-GPI polypeptide D12345 at a dose of 12 mg/kg body weight per day and 250 μL recombinant D1 polypeptide or Fc (control) at a dose of 5.85 mg/kg body weight per day were given daily by peritumoral injection for 9 days. Tumor volume was measured on days 1, 3, 5, 7, and 9. On day 9, mice were killed and tumors were excised, photographed, and weighed.

2.9 | Structural analysis

Sequence similarity between D1 and D2/D3/D4 polypeptides was assessed using a tool, ClustalW, based on their amino acid sequences and compared in terms of sequence conservation.[22] Information of conservation score was used to identify the conserved and nonconserved regions of the polypeptides. To explore the structural properties of β_2-GPI D1, Dictionary of Secondary Structure of Proteins (DSSP) program[23] was used to calculate the solvent accessible surface area (SASA) value and annotate the secondary structure (SS) classes based on amino acid residues obtained from Protein Data Bank, entry ID 1QUB.[24] The information obtained from SASA and SS showed the structural characteristics of β_2-GPI D1, D2, D3, and D4 polypeptides. Root mean square deviations (RMSD) analysis for the tertiary structures of fragments A and B were compared among different polypeptides using PyMol software (https://www.schrodinger.com/suites/pymol), and the structural alignment between D2/D3, D2/D4, and D3/D4 was compared. Evolutionary conservation of β_2-GPI D1 amino acid residues and electrostatic environment of target amino acids were analyzed using CONSURF software (http://consurf.tau.ac.il). Similarity between amino acids was reflected in the substitutions matrix.[25] Sequence alignment between human and mouse β_2-GPI amino acid sequences was compared by the sequence alignment tool, EMBOSS Needle (https://www.ebi.ac.uk/Tools/psa/emboss_needle/). Amino acid mutations and their structural changes in the interaction between D1 and membrane protein annexin A2 (anxA2) were analyzed by the PIPER module of Schrödinger Suite (https://www.schrodinger.com/piper).

2.10 | Immunofluorescence staining

B16-F10 cells (1×10^5 cells/mL) were grown on 18 mm^2 glass coverslips at 37°C under 5% CO_2 for 24 hours with or without purified-β_2GP1 (200 μg/mL), and then fixed with 4% paraformaldehyde at room temperature for 10 minutes. After fixation, cells were washed with PBS buffer, and blocked with 5% BSA in PBS, then incubated with primary antibodies at 4°C overnight or incubated with 1 μg/mL DAPI at room temperature for 10 minutes. After washing with PBS buffer three times, secondary antibody was added and the coverslips were mounted on slides. The cells were visualized using an Olympus BX61 fluorescence microscope.

2.11 | Coimmunoprecipitation assay

B16-F10 cells were seeded in 10-cm dishes at a density of 5×10^5 cells/dish and incubated for 36 hours. For the coimmunoprecipitation assay, membrane protein was extracted and quantified using a Bio-Rad protein assay (Bio-Rad Laboratories). Equal amounts of protein was coimmunoprecipitated with mouse monoclonal antibody against human β_2-GPI (Bethyl Laboratories, Montgomery, TX, USA) or mouse monoclonal antibody against human anxA2 (Santa Cruz Biotechnology, Dallas, TX, USA) at 4°C overnight, and then incubated with protein A/G (1:1) magnetic Sepharose beads (GE Healthcare, Chicago, IL, USA) at 4°C. Mouse IgG (GeneTex, Irvine, CA, USA) was applied as a negative control in the coimmunoprecipitation assay. To elute the bound proteins, 100 mmol/L glycine-HCl (pH 2.8) was added, and the protein complex was resuspended in SDS buffer for SDS-PAGE and western blot analysis as previously described.

2.12 | Site-directed mutagenesis

Residue mutations of β_2-GPI cDNA were constructed by PCR using the QuickChange Lightning site-directed mutagenesis kit (Agilent Technologies, Santa Clara, CA, USA) according to the manufacturer's instructions. Table S2 shows the primers for cDNA synthesis and the corresponding amino acid residues used in site-directed mutagenesis. Each cDNA construct was confirmed by DNA sequencing.

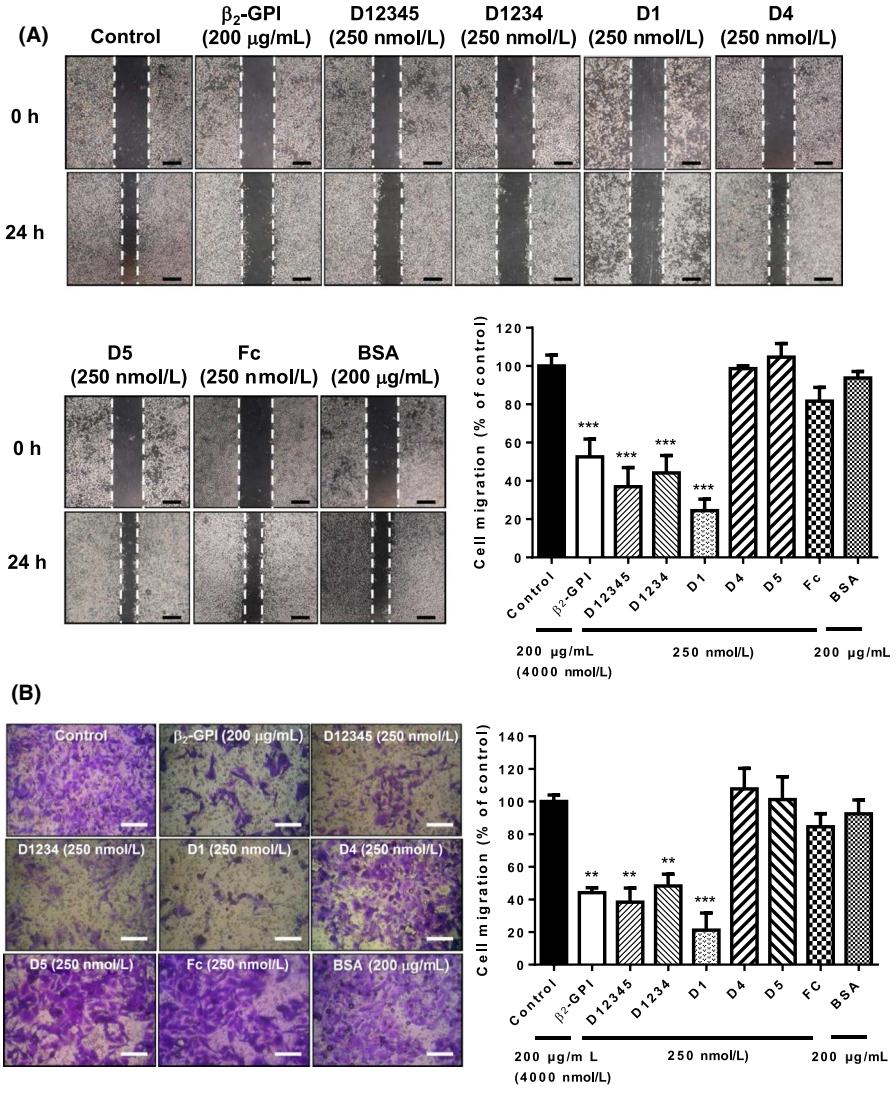

FIGURE 1 Purified β_2-glycoprotein I (β_2-GPI) and recombinant β_2-GPI polypeptides contribute to anti-cell migration. B16-F10 melanoma cells were cultured in 6-well plates at a density of 1.8×10^5 cells/well and treated with the indicated concentrations of purified β_2-GPI, recombinant D1, D4, D5, D1234, and D12345 polypeptides, Fc vector, and BSA (control) for 48 h. A, B16-F10 cells were scraped using a pipette tip (white dotted lines indicate the scratched edges) and the migrating cells were assessed by wound-healing assay at 0 and 24 h. Representative photographs are shown using the inverted phase microscope at 40× magnification. The wound areas were assessed between 0 and 24 h and are represented as the percentage of the control group (set as 100%). ***$P < .001$. B, The effects of purified β_2-GPI and its recombinant polypeptides on anti-melanoma cell migration were also determined by transwell migration assay. Graph shows changes in cell migration as a percentage of the control group. Data represent mean ± SEM of triplicates. **$P < .01$, ***$P < .001$

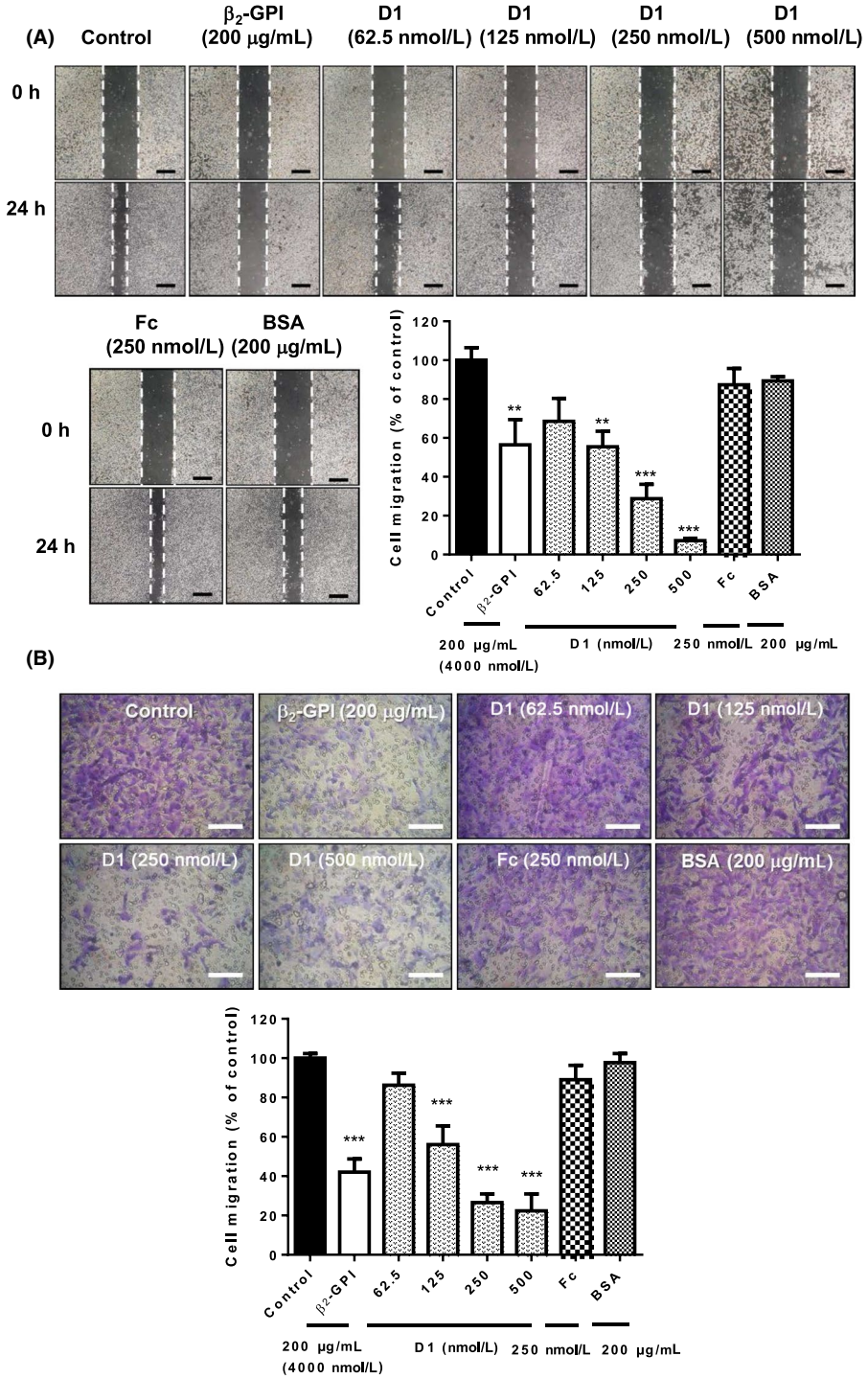

FIGURE 2 Role of recombinant β_2-glycoprotein I (β_2-GPI) D1 polypeptide in the inhibition of melanoma cell migration. B16-F10 melanoma cells were cultured in 6-well plates and treated with or without the indicated concentrations of purified β_2-GPI, recombinant D1 polypeptide, Fc vector, and BSA (control) for 48 h. A, Cells were scraped with a pipette tip (white dotted lines indicate the scratched edges) and the migrating cells were assessed by wound-healing assay. Representative photographs are shown using an inverted phase microscope at 40× magnification. The wound areas between 0 and 24 h were calculated and represented as a percentage of the control group (set as 100%). Graph shows the relative wound width. Data represent mean ± SEM (three individual experiments). $^{**}P < .01$, $^{***}P < .001$. B, Transwell migration assays using B16-F10 cells at different doses of recombinant β_2-GPI D1 polypeptide are shown. Changes in cell migration were also represented as a percentage of the control group. Data represent mean ± SEM of triplicates. $^{***}P < .001$

2.13 | Statistical analysis

Results are expressed as mean ± SEM of at least three independent experiments. Student's *t*-test was used to evaluate statistically significant differences between two groups. Statistical analyses between three or more groups were carried out using one-way ANOVA with Tukey's method as a post-hoc test. $P < 0.05$ was considered statistically significant.

3 | RESULTS

3.1 | Purified β_2-GPI and recombinant β_2-GPI polypeptides suppress B16-F10 melanoma cell migration

We investigated the effects of the purified β_2-GPI and recombinant polypeptides of full-length β_2-GPI (D12345), β_2-GPI domains I-IV (D1234), domain I (D1), domain IV (D4), and domain V (D5) on

B16-F10 cell migration using wound healing (Figure 1A) and transwell migration (Figure 1B) assays. Our results showed that 200 μg/mL (4000 nmol/L) purified β_2-GPI and 250 nmol/L recombinant polypeptides of D12345, D1234, and D1 inhibited B16-F10 cell migration. In contrast, recombinant polypeptides of D4 and D5 had little effect on cell migration. We also evaluated the dose-effect of recombinant peptide D1 on cell migration. Giving 200 μg/mL β_2-GPI and 125-500 nmol/L D1 significantly inhibited wound healing (Figure 2A) and transwell migration (Figure 2B). Furthermore, D1 remarkably reduced melanoma cell migration in a dose-dependent way compared with the controls.

3.2 | Purified β_2-GPI and recombinant β_2-GPI polypeptides inhibit cell proliferation and invasion

To confirm the suppression effect of β_2-GPI on melanoma cell proliferation, cell numbers were counted after treating cells with purified β_2-GPI and recombinant polypeptides for 24, 36, and 48 hours (Figure 3A), and DNA synthesis was assessed by BrdU incorporation assay after treating cells with the purified β_2-GPI and polypeptides for 48 hours (Figure 3B). Cell growth rates of the β_2-GPI, D1234, D12345, and D1-treated groups were slower than those of cells treated with D4 and D5 polypeptides for 24, 36, and 48 hours. Among the tested

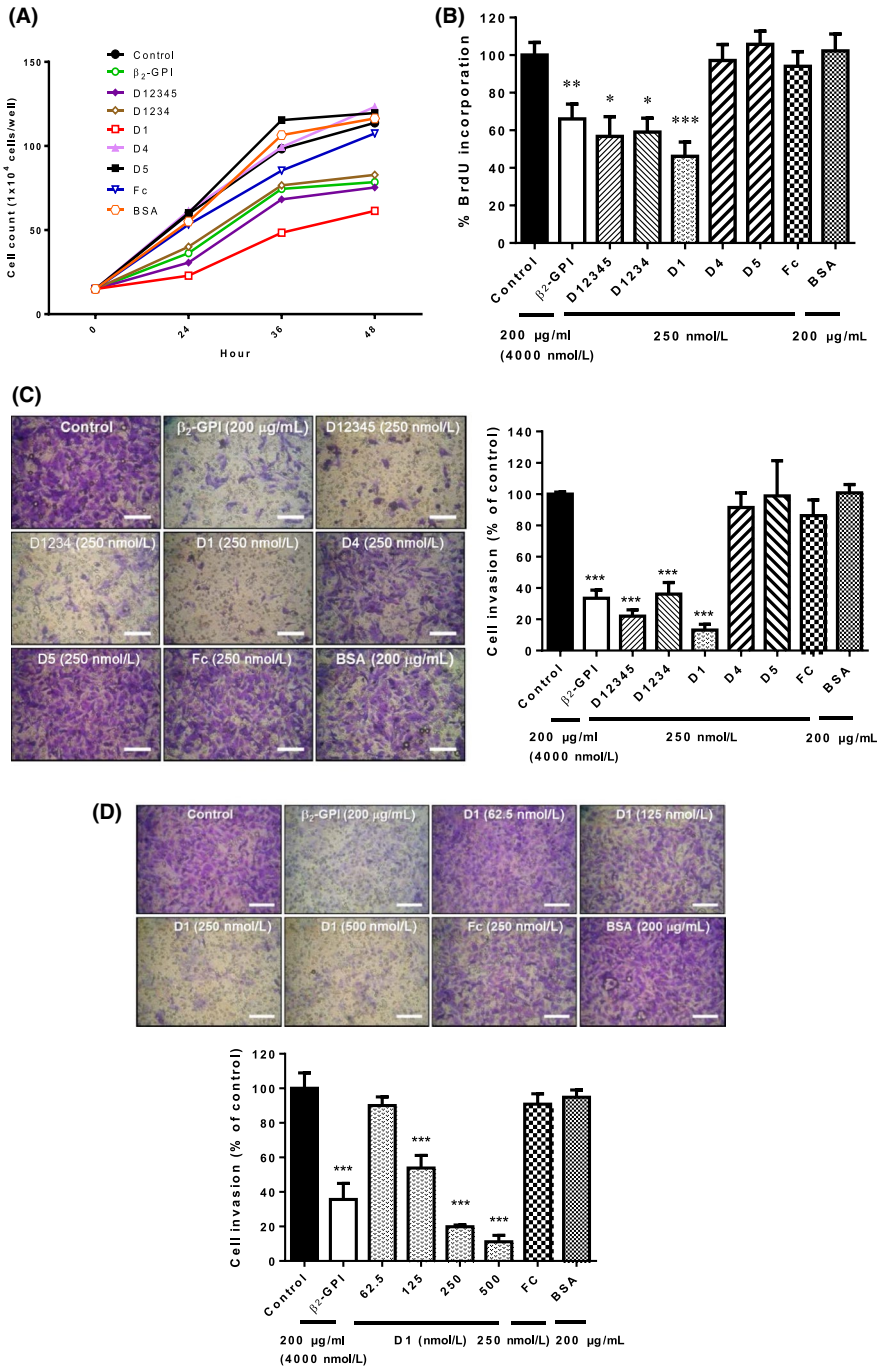

FIGURE 3 Purified β_2-glycoprotein I (β_2-GPI) and recombinant β_2-GPI D1 polypeptide contribute to anti-cell proliferation. B16-F10 melanoma cells were cultured and treated with purified β_2-GPI, recombinant peptides, Fc vector, or BSA (control). A, Cell proliferation was determined using a cell counting assay and cell numbers were scored at 24, 36, or 48 h. B, Cell proliferation was assessed by BrdU incorporation at 24 h. C, B16-F10 melanoma cells were cultured and treated with the indicated concentrations of purified β_2-GPI, recombinant peptides, Fc vector, and BSA (control) for 24 h by invasion analysis. Experiments were repeated three times. Representative images from one experiment are shown (top) and cell invasion was quantified (bottom). D, Invasion assay using B16-F10 cells at different doses of recombinant β_2-GPI D1 polypeptide were assessed. Data represent mean ± SEM of three individual experiments. *P < .01, **P < .01, ***P < .001

polypeptides, D1 showed the most potent inhibition of cell proliferation as determined by cell counting and BrdU assays. Next, we assessed whether β_2-GPI, D1234, D12345, and D1 reduced melanoma cell invasion using a Matrigel-coated invasion assay (Figure 3C). Cells treated with β_2-GPI, D1234, D12345, and D1 showed lower levels of cell invasion compared with the D4 and D5 groups. Furthermore, β_2-GPI D1 inhibited cell invasion in a dose-dependent way. Significant suppression was found in 125, 250, and 500 nmol/L D1-treated cells compared with control cells ($P < .001$) (Figure 3D). Our results indicate that D1 is the most potent recombinant polypeptide reducing proliferation and invasion in B16-F10 melanoma cells.

3.3 | Effects of β_2-GPI and recombinant β_2-GPI polypeptides on protein expression

To determine the underlying mechanisms regulated by β_2-GPI and recombinant β_2-GPI polypeptides, levels of protein expression were determined by western blotting analysis. As shown in Figure 4A, protein levels of p-Akt, p-ERK, and p-p38 were downregulated in cells treated with β_2-GPI, D12345, and D1, whereas the expression of p-JNK was unchanged. Evaluating the NF-κB pathway components, we found that phosphorylation of IKKα and IκBα was significantly reduced by β_2-GPI, D12345, and D1 treatment (Figure 4B). Additionally, nuclear level of p50 expression was also decreased in cells treated with D12345 and D1, but nuclear p65 expression was not affected.

3.4 | β_2-Glycoprotein I and D1 polypeptide suppress melanoma growth in vivo

To validate the antitumor effects of β_2-GPI protein in vivo, we use a syngeneic murine melanoma model to confirm the inhibitory effects of β_2-GPI and its recombinant D1 polypeptide on tumor growth. Mice were killed and tumors were surgically removed for analysis. Tumor volume in the β2-GPI-, D12345-, and D1-treated groups was reduced to 38.4%, 41.8%, and 22.5%, respectively, compared with the control mice at day 9 after treatment (Figure 5A). Significant suppression of the tumor mass was found in β_2-GPI and recombinant D1 groups (Figure 5B). Furthermore, tumors in the D1-treated mice grew much more slowly than those in the other treated mice. These results are in accordance with our findings in vitro.

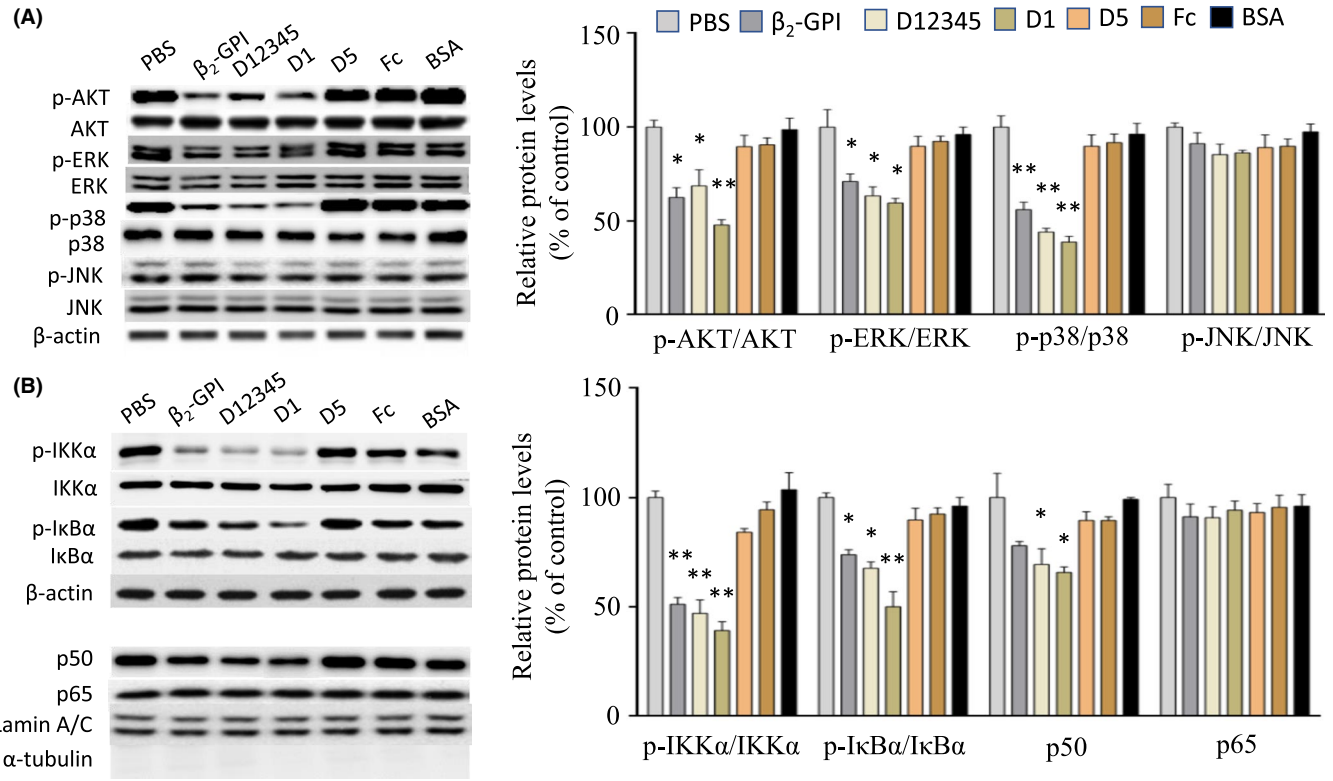

FIGURE 4 Effects of β_2-glycoprotein I (β_2-GPI) and its recombinant polypeptides on protein expression in B16-F10 cells treated with β_2-GPI or recombinant polypeptides. Western blotting analysis for the expression of (A) p-AKT, AKT, p-ERK, ERK, p-p38, p38, p-JNK, and JNK and (B) p-IKKα, IKKα, p-IκBα, IκBα, and the nuclear levels of p50 and p65. β-Actin and lamin A/C were used as the cytosolic and nuclear protein loading control, respectively. α-Tubulin was used to rule out contamination of cytosolic protein in nuclear protein extraction. Representative gels are shown (left) and the intensity of protein bands normalized by the internal control was quantitated as relative protein expression using ImageQuant software (right). Data are presented as mean ± SEM of at least three independent experiments. $^*P < .05$, $^{**}P < .01$ vs control group

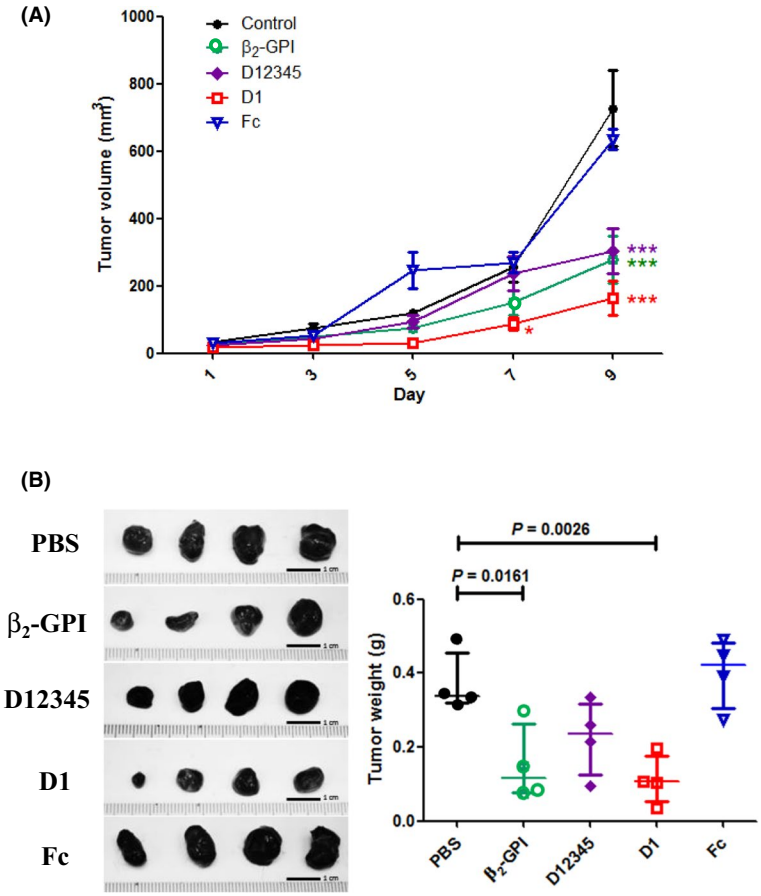

FIGURE 5 Role of purified β_2-glycoprotein I (β_2-GPI) and recombinant polypeptides in melanoma growth. A syngeneic murine melanoma model was established in C57BL6 mice by implanting 5×10^6 B16-F10 melanoma cells/250 μL PBS into the dorsal flanks of each mouse. When tumors reached 100 mm^3, purified β_2-GPI and recombinant polypeptides D12345 and D1 were injected s.c. beside the tumors and the mice were killed on day 9. A, Comparison of tumor growth following injection of purified β_2-GPI, recombinant polypeptides D1 and D12345, and PBS (mock). Tumor volumes were measured using a Vernier caliper every 2 days and were calculated using the formula: length (mm) × width^2 (mm^2) × 0.5. There were four mice per group and tumor volumes are plotted as means ± SEM. B, Mice were killed and the tumors were excised and photographed. Fc represents mice bearing tumors with empty vector. Tumor weights from mice injected with purified β_2-GPI, recombinant polypeptides D12345 and D1, and Fc protein were determined at the end of the experiment. Data representing medium and interquartile range are shown as horizontal lines

3.5 | Sequence-based comparison of the structure of D1 polypeptide and other β_2-GPI domains

Amino acid sequences of the four domains of β_2-GPI were aligned to analyze the structural characteristics of D1-D4 polypeptides (Figure 6A). D1 was found to have less sequence similarity compared with the other three domains (D2, D3, and D4), particularly in fragments A and B. Solvent accessibility results showed that fragments A and B contained higher SASA values within D1 (Figure 6B). The average SASA value for D1 was 40.25. Higher SASA values indicate hydrophilic regions, whereas lower SASA values indicate hydrophobic regions. Regions with higher SASA values and random coil residues were exposed at the surface of the D1 tertiary structure. RMSD values of fragments A and B between D1 and D2, D1 and D3, and D1 and D4 are shown in Figure 6C,D, respectively. Higher RMSD values indicate a less conservative comparative structure. Superimposed topology comparison showed that fragments A and B of D1 were distinctive compared with the corresponding regions of D2, D3, and D4. Structural alignment between D2/D3, D2/D4, and D3/D4 are shown in Figure S2. RMSD values of D2/D3, D2/D4, and D3/D4 were 1.168, 0.980, and 1.105 Å, respectively. It seems that D2 has the highest similarity (with lowest RMSD value) of structural conformation with D4. Sequence identity between human and mouse β_2-GPI is 76.5% and the similarity between the two polypeptides is 87.2% (Figure S3). This shows that the protein structure of human and mouse β_2-GPI are highly conserved.

3.6 | Validation of the hotspots in fragments A and B of D1 polypeptide

Based on the results of structural comparisons between D1 and D2/D3/D4 polypeptides, five amino acids P11, P17, K19, M42 and I55 in fragments A and B of the D1 polypeptide were proposed as

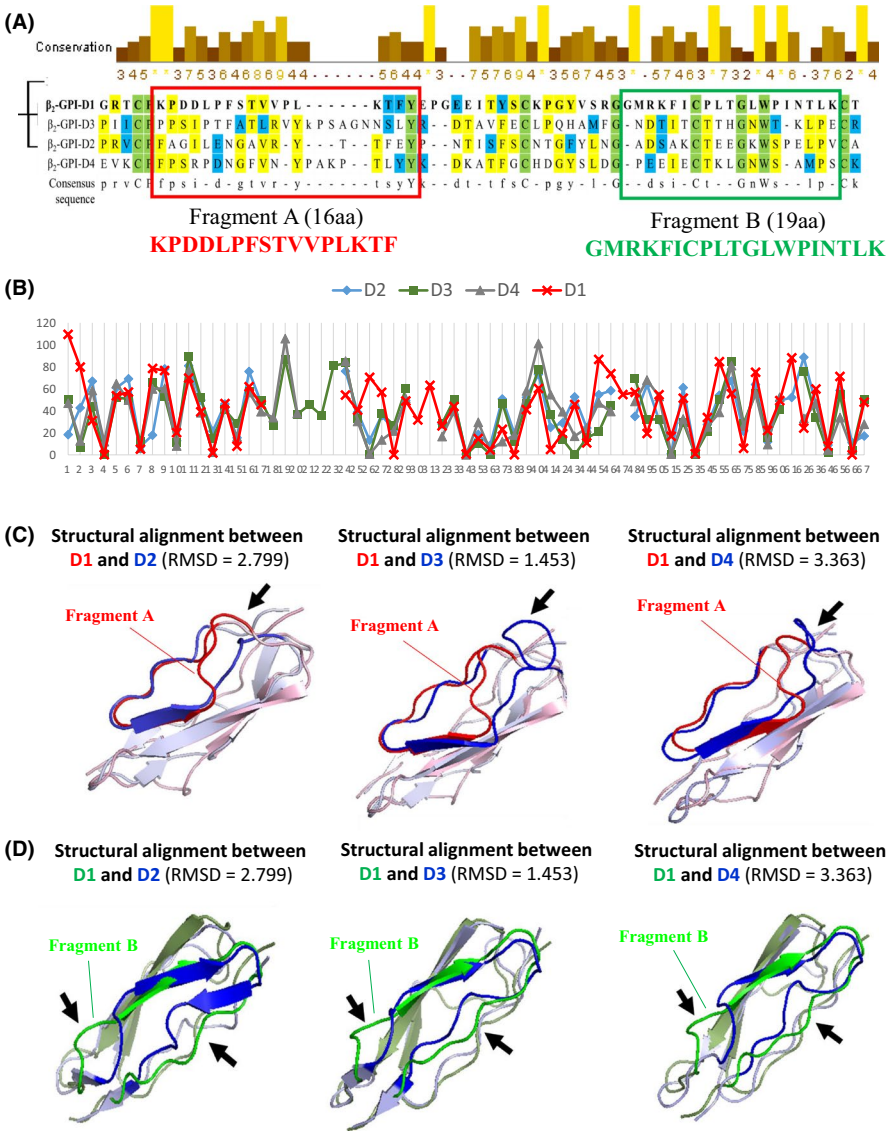

FIGURE 6 Structural comparison of β_2-glycoprotein I (β_2-GPI) D1 polypeptide and other β_2-GPI domains. A, Comparison of sequence conservation between D1 and D2/D3/D4 polypeptides was carried out using the multiple sequence alignment (MSA) tool, ClustalW. Bar chart represents the degree of conservation at each amino acid position. Higher conservation scores are represented by higher bars colored with yellow. The amino acids colored with green show completely conserved residues, yellow indicates identical residues, and blue highlights residues with similar physicochemical properties. The lower line of the alignment is the consensus sequence. Fragment A (amino acids 6-21) and fragment B (amino acids 41-59) are the peptide regions with lowest similarity between D1 and D2/D3/D4 polypeptides. B, Solvent accessible surface area (SASA) and secondary structure (SS) were calculated using Dictionary of Secondary Structure of Proteins (DSSP) program[23] program to estimate the structural characterization of D1 (red), D2 (blue), D3 (green) and D4 (gray). In the line graph, the *Y*-axis represents the relative area (%) of solvent accessibility and the *X*-axis represents the position of the amino acid residues. C,D, Structure comparison of fragments A (red) and B (green) of D1 illustrated as superimposed on the corresponding moieties of other peptide regions (blue) in D2, D3, and D4. Root mean square deviation (RMSD) using PyMol software was carried out. Black arrows show the distinctive regions of fragments A and B compared with the corresponding region (blue line) in the D2, D3, and D4 structures

the possible binding hotspots to interact with the counterpart molecules. Figure 7A shows that the five amino acids are located in the coil regions; however, P11 and P17 are close to the β2 strand, and M42 is close to the β5 strand in the D1 structure. I55 is the most variable among the five amino acids using evolutionary conservation analysis. In contrast, K19 is located in a conserved position (Figure 7B). Furthermore, all of the five amino acid residues are located in the surface area of the D1 tertiary structure (Figure 7C). According to the electrostatic surface representation, P17, K19, M42 and I55 are shown to be located in a highly electropositive environment (Figure 7D), which may interact with the basic residues of other interacting proteins.

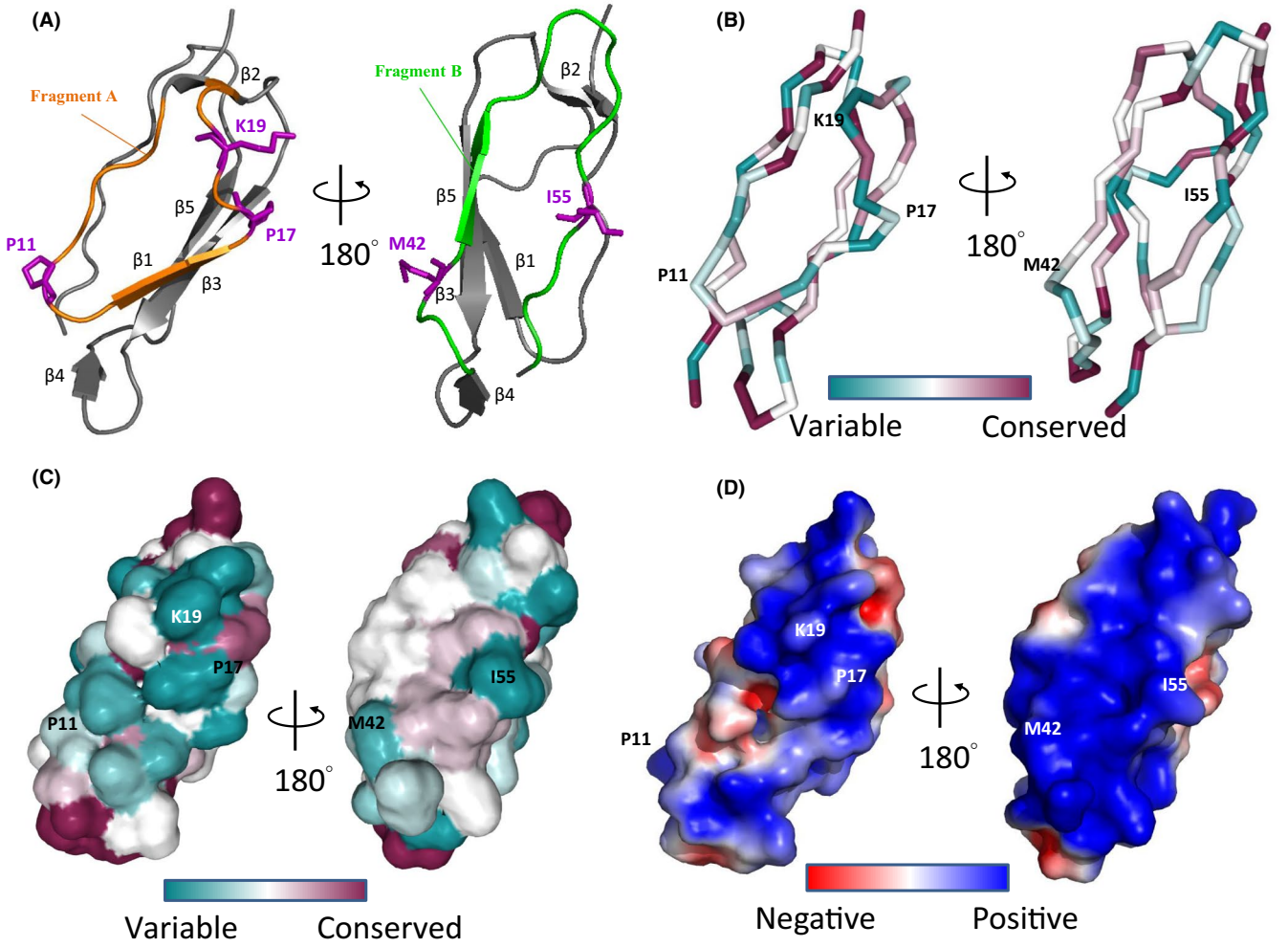

FIGURE 7 Hotspot detection in fragments A and B of β_2-glycoprotein I (β_2-GPI) D1 polypeptide. A, Five nonconservative amino acid residues (P11, P17, K19, M42, and I55) are represented in purple in the illustration based on the PyMOL visualization of PDB ID 1QUB. The view for visualizing P11, P17, and K19 residues in fragment A (orange) is rotated 180° around the vertical axis for visualizing M42 and I55 residues in fragment B (green). B, Evolutionary conservation analysis was done using CONSURF software based on the secondary structure of fragments A and B. The conservation scores are divided into nine grades for visualization, from the most variable positions colored cyanine, through the intermediately conserved positions colored white, to the most conserved positions colored purple. C, Surface information was incorporated into the 3-D structure of fragments A and B, colored from cyanine (variable) to purple (conserved), based on the analysis by CONSURF software. D, Using the default parameters in the CONSURF package, electrostatic surface representation of fragments A and B, colored red to blue from −5.5 to +5.5 kT/e, was conducted to explore the electrostatic environment around the five amino acids on the surface area of D1 polypeptide

3.7 | β_2-Glycoprotein I and D1 polypeptide interact with annexin A2 in melanoma cells

To determine which protein is the counterpart molecule of β_2-GPI, we determined the partner protein of β_2-GPI by immunofluorescence staining, coimmunoprecipitation assay, and molecular docking approaches. Double immunofluorescence staining showed β_2-GPI and anxA2 coexpression on the B16-F10 cell membrane (Figure 8A). Direct interaction between β_2-GPI and anxA2 was further confirmed by coimmunoprecipitation assay as shown in Figure 8B. To define the possible binding site of β_2-GPI D1 on the cell membrane, we used a molecular docking strategy to clarify several amino acid residues of D1 and found that P11, M42, and I55 residues allow a closer conformation distance with anxA2 (Figure 8C). G250 and R284 residues of anxA2 are the closest counterpart toward D1 structure. However, mutation of P11, M42 and I55 residues disrupt the structural stability between β2-GPI D1 and anxA2. From analysis using the PIPER module of the Schrödinger Suite, binding affinity between mutated β2-GPI D1 and anxA2 was decreased to −18.13 kcal/mol after mutations of P11A, M42A, and I55P. As shown in Figure 8D, mutation of the three amino acid sites obviously diminished the hydrogen-bond interaction between β2-GPI D1 and anxA2. The structure-function relationship of the five selected amino acids was clarified further by site-directed mutagenesis. Mutation of P11A, M42A, and I55P reversed the cell migration ability of D1 on melanoma cell migration, whereas mutation of P17Y and K19T did not affect cell migration (Figure 8E). Therefore, P11A, M42A, and I55P residues are likely the key hotspots in the

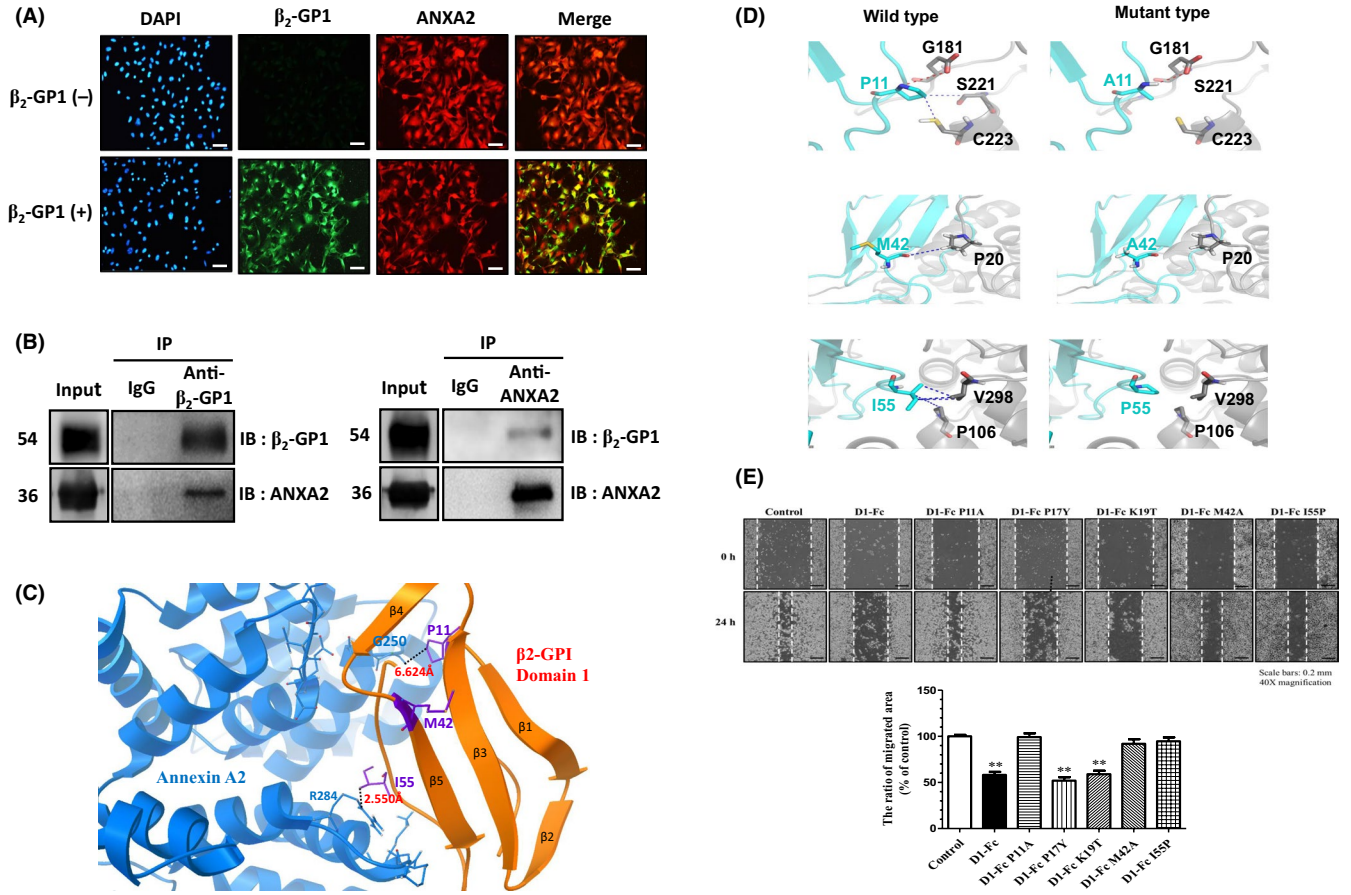

FIGURE 8 Molecular counterpart of β_2-glycoprotein I (β_2-GPI) and the functional importance of β_2-GPI D1 hotspot. A, Representative immunofluorescence images of B16-F10 cells stained for β_2-GPI (green) and annexin A2 (red). Merged image of β_2-GPI and annexin A2 staining cells is shown in yellow. Cell nuclei were stained with DAPI (blue). Scale bar, 50 μm. B, Interaction of β_2-GPI and annexin A2 was confirmed by coimmunoprecipitation (co-IP) experiment. Cells were lysed and membrane protein extracts were immunoprecipitated with anti-β_2GP1 (left) or anti-annexin A2 (right) antibody, followed by immunoblotting with anti-β_2GP1 or anti-annexin A2. C, Interactions between the amino acid residues of annexin A2 (blue) and β2-GPI D1 (orange) are illustrated. The figures of the structures depicted were retrieved from Protein Data Bank and PyMol software. Hydrogen-bond interactions between amino acids of D1 and annexin A2 are shown as black dashed lines. D, Close view of amino acid interaction between β2-GPI D1 (cyan) and annexin A2 (gray) is analyzed by using the PIPER module of Schrödinger Suite (https://www.schrodinger.com/). Structural changes in mutant-type amino acids P11A, M42A, and I55P were compared with wild-type amino acids. E, Residue mutations of β_2-GPI cDNA were constructed by site-directed mutagenesis. Then, B16-F10 cells were scraped with a pipette tip and treated with D1, D1 P11A, D1 P17Y, D1 K19T, D1 M42A, or D1 I55P, and functional analysis of site mutation was detected by migration assay. Representative photographs are shown at 40× magnification. Scale bars represent 0.2 mm. Percentage of the migrating area was calculated as: 100% − (wound areas at 24 h/wound areas at 0 h) × 100% and represented as a percentage of the control. Data represent mean ± SEM of at least three independent experiments. $^{**}P < .01$ compared with the control

D1 polypeptide that are involved in the function of anti-melanoma cell migration.

4 | DISCUSSION

Several studies have characterized cell migration and proliferation in the progression of tumorigenesis.[12-15] We showed previously that purified β_2-GPI inhibits cell migration, proliferation, and angiogenesis in human aortic endothelial cells.[9-11] However, the role of natural β_2-GPI in tumor development remains unknown. The present study showed that β_2-GPI is a negative regulator of cell migration, proliferation, and invasion in melanoma cells. Furthermore, we analyzed the structure-function relationship of different β_2-GPI domains involved in the control of tumor development.

It has been shown that the N-terminal domains of β_2-glycoprotein I (DI-IV) inhibit VEGF- and basic fibroblast growth factor-induced angiogenesis in human umbilical vein cells.[26] However, domain V at the C-terminus differs from DI-IV in that it is critical for phospholipid binding.[27,28] The plasmin-nicked form of β_2-GPI was also identified to have antiangiogenic effects in endothelial cells.[29] Recently, enhanced microvessel formation and melanoma tumor growth were identified in β_2-GPI-deficient mice.[30] To determine the precise role of β_2-GPI in the regulation of melanoma cell migration, cell proliferation, and tumor growth, we carried out in vitro and in vivo experiments using purified β_2-GPI and its recombinant peptide domains.

Additionally, structural characteristics were revealed using various bioinformatics-based analyses.

Recombinant polypeptides of β_2-GPI D12345 (full length), D1234, D1, D4, D5 were generated using the Bac-to-Bac Baculovirus Expression System. Administration of recombinant polypeptides D12345, D1234, and D1 significantly inhibited cell migration, proliferation, and invasion in B16-F10 melanoma cells. Potency of 250 nmol/L polypeptides D12345 and D1 was even stronger than the average concentration (200 μg/mL) of native β_2-GPI. Furthermore, D1 peptide showed the most potent inhibitory activities in tumor cells. Therefore, we speculate that the D1 polypeptide is a powerful suppressor of tumor growth in animals. Consistent with the cell culture results, potent suppression of melanoma growth (77.5% inhibition) was observed in mice treated with recombinant D1 polypeptide. Cancer progression involves the regulation of many genes and different signaling pathways.[31,32] Here, we also elucidated the possible β_2-GPI-mediated molecular mechanisms by western blot analysis. Alterations of AKT, ERK1/2, p38, and NF-κB activation are known in tumorigenesis.[31-34] We thus expect that β_2-GPI and D1 polypeptide may regulate these signaling pathways and consequently inhibit melanoma cell migration, cell proliferation, and tumor growth.

In a previous study, anxA2 was reported to bind with β_2-GPI in patients with cerebral venous thrombosis.[35] Clinical studies have shown that anxA2 is highly expressed in different tumor types.[36,37] Accordingly, recent reports have shown the functional role for anxA2 in regulation of cell adhesion, migration, and invasion.[38,39] In the present study, binding of β_2-GPI to anxA2 was confirmed by immunofluorescence and coimmunoprecipitation assays. Furthermore, interaction between specific amino acids of β_2-GPI D1 and anxA2 was shown by the molecular docking approach. Although anxA2 may be considered a molecular target of β_2-GPI in melanoma cells, the clinical implications of our findings remain elusive. Further studies are needed to determine the exact mechanism of β_2-GPI-mediated anxA2 regulation in melanoma progression.

Many bioinformatics tools have been used to elaborate the structural characteristics attributable to the biological function of proteins. Results of multiple sequence alignments highlighted the possible functional importance of fragments A and B within β2-GPI D1. A spatially superimposed comparison of the tertiary structures of D1 with other β_2-GPI domains provided structural uniqueness in fragments A and B. Results of molecular simulation indicate that amino acid substitutions of P11, M42, and I55 residues of D1 polypeptide change the hydrogen-bond interaction between D1 polypeptide and anxA2. Furthermore, results of site-directed mutagenesis are sufficient to show that the three nonpolar amino acids, P11, M42 and I55 within fragments A and B were crucial for anti-melanoma cell migration.

Both molecular simulation and site-directed mutagenesis assays provide us with coincident evidence for the essential amino acid residues of D1 polypeptide, which may trigger intracellular signaling pathways and consequently modulate tumor malignancy. An additional possibility is that other amino acid residues on the tertiary surface of β_2-GPI also interact with membrane receptors other than anxA2, which could contribute to the prevention of cancer progression. Future work is needed to address these possibilities. Taken together, this study shows the molecular basis of the structure-function relationship between D1 polypeptide and melanoma progression. The combination of structural, biochemical, and functional insights presented here provides strong expectation that D1 of β_2-GPI may represent a new medication warranting further preclinical investigation for anticancer therapy.

ACKNOWLEDGMENT

This study was supported by grants (MOST103-2320-B-010-024-MY3, MOST106-2320-B-010-028, MOST107-2320-B-010-035) from the Ministry of Science and Technology, ROC (Taiwan).

DISCLOSURE

Authors declare no conflicts of interest for this article.

ORCID

An-Na Chiang https://orcid.org/0000-0003-4177-6166

REFERENCES

1. Lozier J, Takahashi N, Putnam FW. Complete amino acid sequence of human plasma beta2-glycoprotein I. *Proc Natl Acad Sci USA*. 1984;81:3640-3644.
2. Schwarzenbacher R, Zeth K, Diederichs K, et al. Crystal structure of human beta2-glycoprotein I: implications for phospholipid binding and the antiphospholipid syndrome. *EMBO J*. 1999;18:6228-6239.
3. Radic M, Pattanaik D. Cellular and molecular mechanisms of anti-phospholipid syndrome. *Front Immunol*. 2018;9:969.
4. He C, Zhang G, Zhou H, Cheng S, Farwa A. Effects of Toll-like receptor 4 on β_2-glycoprotein I-induced splenic T cell subsets differentiation. *Immunol Lett*. 2018;198:17-25.
5. Amengual O, Atsumi T. Antiphospholipid syndrome, "the best prophet of the future". *Mod Rheumatol*. 2018;28:409-416.
6. Chighizola CB, Pregnolato F, Andreoli L, et al. Beyond thrombosis: anti-β2GPI domain 1 antibodies identify late pregnancy morbidity in anti-phospholipid syndrome. *J Autoimmun*. 2018;90:76-83.
7. Pozzi N, Acquasaliente L, Frasson R, et al. β_2-Glycoprotein I binds to thrombin and selectively inhibits the enzyme procoagulant functions. *J Thromb Haemost*. 2013;11:1093-1102.
8. Ioannou Y, Zhang JY, Passam FH, et al. Naturally occurring free thiols within beta$_2$-glycoprotein I in vivo: nitrosylation, redox modification by endothelial cells, and regulation of oxidative stress-induced cell injury. *Blood*. 2010;116:1961-1970.
9. Chiu WC, Chiou TJ, Chiang AN. β_2-Glycoprotein I inhibits endothelial cell migration through nuclear factor κB signaling pathway and endothelial nitric oxide synthase activation. *Biochem J*. 2012;445:125-133.
10. Chiu WC, Lin JY, Lee TS, You L, Chiang AN. β_2-Glycoprotein I inhibits VEGF-induced endothelial cell growth and migration via suppressing phosphorylation of VEGFR2, ERK1/2 and Akt. *Mol Cell Biochem*. 2013;372:9-15.
11. Chiu WC, Chiou TJ, Chung MJ, Chiang AN. β_2-glycoprotein I inhibits vascular endothelial growth factor-induced angiogenesis by suppressing the phosphorylation of extracellular signal-regulated

kinase 1/2, Akt, and endothelial nitric oxide synthase. *PLoS ONE*. 2016;11:e0161950.
12. Chen J, Hao Y, Chen J, et al. Colony stimulating factor-1 receptor promotes proliferation, migration and invasion in the human nasopharyngeal carcinoma 6-10B cell line via the phosphoinositide 3-kinase/Akt pathway. *Oncol Lett*. 2018;16:1205-1211.
13. Liu Y, Zhou H, Ma X, et al. Prodigiosin inhibits proliferation, migration, and invasion of nasopharyngeal cancer cells. *Cell Physiol Biochem*. 2018;48:1556-1562.
14. Monisha J, Roy NK, Padmavathi G, et al. NGAL is downregulated in oral squamous cell carcinoma and leads to increased survival, proliferation, migration and chemoresistance. *Cancers*. 2018;10:228.
15. Shi H, Shi J, Zhang Y, et al. Long non-coding RNA DANCR promotes cell proliferation, migration, invasion and resistance to apoptosis in esophageal cancer. *J Thorac Dis*. 2018;10:2573-2582.
16. Gao Z, Liu R, Ye N, et al. FOXO1 inhibits tumor cell migration via regulating cell surface morphology in non-small cell lung cancer cells. *Cell Physiol Biochem*. 2018;48:138-148.
17. Lou Z, Lee BS, Ha T, et al. ESE-1 suppresses the growth, invasion and migration of human NSCLC cells and tumor formation in vivo. *Oncol Rep*. 2018;40:1734-1742.
18. Xu W, Xu J, Wang T, et al. Ellagic acid and Sennoside B inhibit osteosarcoma cell migration, invasion and growth by repressing the expression of c-Jun. *Oncol Lett*. 2018;16:898-904.
19. Siegel RL, Miller KD, Jemal A. Cancer statistics, 2017. *CA Cancer J Clin*. 2017;67:7-30.
20. Sykes EK, Mactier S, Christopherson RI. Melanoma and the unfolded protein response. *Cancers*. 2016;8:E30.
21. Eroglu Z, Ozgun A. Updates and challenges on treatment with BRAF/MEK-inhibitors in melanoma. *Expert Opin Orphan Drugs*. 2018;6:545-551.
22. Larkin MA, Blackshields G, Brown NP, et al. Clustal W and Clustal X version 2.0. *Bioinformatics*. 2007;23:2947-2948.
23. Kabsch W, Sander C. Dictionary of protein secondary structure: pattern recognition of hydrogen-bonded and geometrical features. *Biopolymers*. 1983;22:2577-2637.
24. Bouma B, de Groot PG, van den Elsen JMH, et al. Adhesion mechanism of human beta(2)-glycoprotein I to phospholipids based on its crystal structure. *EMBO J*. 1999;18:5166-5174.
25. Ashkenazy H, Abadi S, Martz E, et al. ConSurf 2016: an improved methodology to estimate and visualize evolutionary conservation in macromolecules. *Nucleic Acids Res*. 2016;44:W344-W350.
26. Yu P, Passam FH, Yu DM, Denyer G, Krilis SA. Beta$_2$-glycoprotein I inhibits vascular endothelial growth factor and basic fibroblast growth factor induced angiogenesis through its amino terminal domain. *J Thromb Haemost*. 2008;6:1215-1223.
27. Sheng Y, Sali A, Herzog H, Lahnstein J, Krilis SA. Site-directed mutagenesis of recombinant human beta 2-glycoprotein I identifies a cluster of lysine residues that are critical for phospholipid binding and anti-cardiolipin antibody activity. *J Immunol*. 1996;157:3744-3751.
28. McNeil HP, Simpson RJ, Chesterman CN, Krilis SA. Anti-phospholipid antibodies are directed against a complex antigen that includes a lipid-binding inhibitor of coagulation: beta 2-glycoprotein I (apolipoprotein H). *Proc Natl Acad Sci USA*. 1990;87:4120-4124.
29. Nakagawa H, Yasuda S, Matsuura E, et al. Nicked β_2-glycoprotein I binds angiostatin 4.5 (plasminogen kringle 1-5) and attenuates its antiangiogenic property. *Blood*. 2009;114:2553-2559.
30. Passam FH, Qi JC, Tanaka K, Matthaei KI, Krilis SA. In vivo modulation of angiogenesis by beta 2 glycoprotein I. *J Autoimmun*. 2010;35(3):232-240.
31. Colombo F, Zambrano S, Alessandra Agresti A. NF-κB, the importance of being dynamic: role and insights in cancer. *Biomedicines*. 2018;6:45.
32. Kamiyama M, Naguro I, Ichijo H. In vivo gene manipulation reveals the impact of stress-responsive MAPK pathways on tumor progression. *Cancer Sci*. 2015;106:785-796.
33. Tarhouni-Jabberi S, Zakraoui O, Ioannou E, et al. Mertensene, a halogenated monoterpene, induces G2/M cell cycle arrest and caspase dependent apoptosis of human colon adenocarcinoma HT29 cell line through the modulation of ERK-1/-2, AKT and NF-κB signaling. *Mar Drugs*. 2017;15:221.
34. Chao W, Deng JS, Li PY, Liang YC, Huang GJ. 3,4-Dihydroxybenzalactone suppresses human non-small cell lung carcinoma cells metastasis via suppression of epithelial to mesenchymal transition, ROS-mediated PI3K/AKT/MAPK/MMP and NFκB signaling pathways. *Molecules*. 2017;22:537.
35. Cesarman-Maus G, Cantú-Brito C, Barinagarrementeria F, et al. Autoantibodies against the fibrinolytic receptor, annexin A2, in cerebral venous thrombosis. *Stroke*. 2011;42:501-503.
36. Esposito I, Penzel R, Chaib-Harrireche M, et al. Tenascin C and annexin II expression in the process of pancreatic carcinogenesis. *J Pathol*. 2006;208:673-685.
37. Shetty P, Bargale A, Patil BR, et al. Cell surface interaction of annexin A2 and galectin-3 modulates epidermal growth factor receptor signaling in Her-2 negative breast cancer cells. *Mol Cell Biochem*. 2016;411:221-233.
38. Staquicini DI, Rangel R, Guzman-Rojas L, et al. Intracellular targeting of annexin A2 inhibits tumor cell adhesion, migration, and *in vivo* grafting. *Sci Rep*. 2017;7:4243.
39. Lokman NA, Ween MP, Oehler MK, Ricciardelli C. The role of annexin A2 in tumorigenesis and cancer progression. *Cancer Microenviron*. 2011;4:199-208.

SUPPORTING INFORMATION

Additional supporting information may be found online in the Supporting Information section at the end of the article.

How to cite this article: Leu S-JJ, Lee T-Y, Cheng S-W, et al. Structural and functional characterization of β_2-glycoprotein I domain 1 in anti-melanoma cell migration. *Cancer Sci*. 2019;110:1974–1986. https://doi.org/10.1111/cas.14030